Soft Matter

PAPER

New strategy of nanolithography *via* controlled block copolymer self-assembly

Nan Xie,[a] Weihua Li,*[a] Feng Qiu[ab] and An-Chang Shi[c]

The self-assembly of block copolymer–homopolymer blends in bulk, as well as under the direction of periodic patterned surfaces, has been investigated by computer simulations of the time-dependent Ginzburg–Landau theory. Specifically, a small amount of homopolymers are added to regulate the spontaneous nucleation rate and substrate patterns are designed to control the position and orientation of the induced nuclei. The mechanism, validity and efficiency of this scheme is examined using 2D and 3D computer simulations of cylinder-forming block copolymer–homopolymer blends, demonstrating that large-scale perfectly ordered patterns can be produced by controlling the position and orientation of induced multiple nucleation events. This scheme, combining the nucleation event of block copolymer self-assembly with the direction of the patterned surface, can be used in the lithography technique of block copolymers to significantly improve the directing efficiency, *i.e.*, the density multiplication.

1 Introduction

The directed self-assembly of block copolymers (BCPs), typically realized by placing BCPs on patterned substrates to form large-scale ordered BCP structures, has attracted considerable attention because it provides a bottom-up platform for nano-lithography. It has been argued that BCP lithography has the potential to overcome the intrinsic limitations of standard photolithography, and to decrease the cost of e-beam lithography of sub-30 nm patterns in semiconductor technologies.[1,2] One of the most investigated techniques to direct BCP self-assembly is graphoepitaxy, which utilizes patterned templates to form large-scale perfectly ordered patterns, particularly in thin films.[1-13] An important parameter in substrate-directed BCP self-assembly is the density multiplication (DM), which can be quantified by the ratio of the number of self-assembled BCP domains to the number of directing substrate domains in a given area or volume of the sample. The DM determines the directing efficiency of the substrate effects. A larger DM means sparser substrate features are required and thus reduces the manufacturing cost. To date, the highest experimentally reported DM for hexagonally arranged BCP cylinders/spheres is about 25.[7] This upper limit of the DM is qualitatively consistent with the theoretical prediction of Li *et al.*[14] based on their time-dependent Ginzburg–Landau (TDGL) simulations. In a recent study using self-consistent mean-field theory, Tang and Ma obtained a theoretical DM of about 34,[15] which is the highest DM presented in the literature. From the ordering mechanism discussed in our previous work,[14] it is apparent that simple substrate patterns will not increase the DM significantly. The limiting factors of the DM are spontaneous nucleation of, and orientation mismatch between, the ordered domains. Specifically, spontaneous nucleation and/or uncontrolled nucleation sites will produce multiple ordered domains with random locations and orientations. The different orientations and locations will lead to a large number of defects such as grain boundaries, dislocations and disclinations when these domains grow and eventually merge. The annihilation of these defects is typically a very slow process, making it virtually impossible to form large-scale ordered samples in this case.[14]

In order to improve the DM, a new scheme addressing these factors must be designed. Specifically, spontaneous nucleation events must be suppressed so that no ordered domains occur at random positions with arbitrary orientations. At the same time, the nuclei of ordered phases must be induced at prescribed positions with coherent orientations so that no defects are created when these ordered domains merge to form a large-scale single crystal. The spontaneous nucleation of the ordered domains is controlled by the intrinsic thermodynamic properties of the block copolymers, whereas the induction of nucleation events can be controlled by specifically designed features of the substrate patterns. In this paper we will demonstrate that a careful adjustment of the thermodynamic conditions and the design of the substrate patterns will lead to the controlled nucleation of coherent nuclei, resulting in the formation of

[a]State Key Laboratory of Molecular Engineering of Polymers, Department of Macromolecular Science, Fudan University, Shanghai 200433, China. E-mail: weihuali@fudan.edu.cn

[b]Key Laboratory of Computational Physical Sciences, Ministry of Education of China, Shanghai 200433, China

[c]Department of Physics and Astronomy, McMaster University, Hamilton, Ontario, Canada, L8S 4M1

perfectly ordered domains over a large area and unprecedented DM values of at least 128. It is well established that, depending on the thermodynamic stability of the disordered phase, the phase transition proceeds *via* two routes.[16–22] When the disordered phase is metastable, the ordered phase emerges *via* nucleation and growth, where nucleation of the stable ordered phase from the metastable disordered phase is a thermally activated process. When the disordered phase is unstable (near or beyond the spinodal line), the ordered phase emerges *via* spinodal decomposition, where small fluctuations are spontaneously amplified to form the ordered phase. Typically, the patterns formed *via* spinodal decomposition have no long-range order due to the spontaneous nature of the process. Therefore the system should be placed in the region of the phase diagram where the disordered phase is metastable, so that nucleation and growth dominate the ordering kinetics.

When the disordered phase of the system is metastable, the formation of the ordered phase is controlled by the nucleation rate, which can be defined by the probability of having one nucleation event in a unit volume per unit time. Furthermore, nucleation events can be divided into two categories; homogeneous nucleation, which is a randomly occurring rare event due to thermal fluctuations, and heterogeneous nucleation, which is an event induced by external means such as foreign particles and substrates. When the rate of homogeneous nucleation is high, multiple nucleation events occur at random locations and the ordered domain due to each nucleus has a random orientation, leading to the formation of polycrystalline samples plagued with defects. Therefore, in order to form large-scale singly crystalline samples, the nucleation rate should be suppressed to prevent the spontaneous formation of multiple domains. Ideally, if we could control the nucleation rate such that there is one, and only one, nucleation event in the sample, then the growth of this nucleus will produce a perfect single crystal provided that further nucleation events do not occur during the growth of the first ordered domain. However, this simple strategy is not practical because it requires an extraordinarily low nucleation rate to ensure that there are no subsequent nucleation events in the growth period. The low nucleation rate in turn requires a very long incubation time. Furthermore, the time and location of the nucleation event is unpredictable in the case of homogeneous nucleation. A simple strategy to overcome this difficulty is to introduce a nucleation agent to the desired position at the desired time, leading to a controlled nucleation event at a specified location and time. This induced nucleus will then grow and occupy the whole macroscopic sample provided that the homogeneous nucleation rate is low enough to prevent the occurrence of further nucleation events. In principle this strategy can produce large-scale ordered samples. However, the growth of the nucleus to occupy the whole sample becomes the limiting factor, so it is desirable to speed up the growth process. In order to overcome the growth limitation, a periodic array of nucleation sites in the form of substrate patterns can be introduced to the system. When the period of the substrate pattern is commensurate with the period of the ordered phase, multiple nuclei are induced at positions which are commensurate with the structure of the ordered phase of the BCPs. The growth of the multiple domains will lead to a shorter growth time, thus

overcoming the drawback of the strategy of using only one nucleus. On the other hand, if only the positions of the nuclei are controlled, the ordered domains can possess different orientations, leading to the formation of polycrystalline samples. This is the major factor limiting the DM to 25–30.

Based on the above observations, a new scheme to produce large-scale perfectly ordered patterns from BCP self-assembly can be obtained by keeping a low homogeneous nucleation rate and, at the same time, controlling the position and orientation of the induced ordered domains. In what follows we will demonstrate the mechanism and validity of this new strategy using time-dependent Ginzburg–Landau simulations of thin films of AB-diblock copolymer–C-homopolymer (AB–C) blends on patterned substrates. We focus on thin films of the blends which form hexagonally packed cylindrical A-domains, which are aligned perpendicular to the substrate. The homopolymer concentration is used to regulate the phase diagram of the system, thus controlling the homogeneous nucleation rate. The substrate patterns are carefully designed to induce multiple nuclei of the ordered domains at desired locations with specified orientations. This new scheme leads to the formation of single-crystalline samples over a large area and an increased DM value of at least 128.

2 Theory and model

Our model system of AB–C blends forms a thin film of perpendicular cylinders on a substrate, thus the system can be simplified to a two-dimensional (2D) one. Because we are interested in the formation of ordered patterns in large systems, the simulation box must be much larger than the size of a single cylinder, such that the number of A-cylinders in the system is of the order 10^4. In order to simulate large systems, a time-dependent Ginzburg–Landau (TDGL) model is adopted in our study. It has been well established that the TDGL model of block copolymers can describe the ordering kinetics of phase separation and phase ordering processes of BCPs.[14,23,24] In particular, a TDGL model has been used to study the nucleation of lamellae from a metastable cylindrical phase.[25] For the case of neat diblock copolymers, the metastability region of the disordered phases is limited.[26] Homopolymers are often added into BCPs to regulate the segregation degree[27,28] and the domain spacing.[29] In the current study we consider binary mixtures of AB diblock copolymers and B-selective C-homopolymers, which are used to regulate the stability of the disordered phase. Specifically, the polymers are characterized by their degrees of polymerization N_k (k = A, B, and C), thus $N = N_A + N_B$ is the total degree of polymerization of the BCPs. The local monomer density at a position $\mathbf{r}$ is denoted as $\phi_k(\mathbf{r})$ (k = A, B, and C), which is the order parameter of the system for each component. The incompressibility condition leads to two independent order parameters, which can be chosen as $\phi(\mathbf{r}) = \phi_A(\mathbf{r}) - \phi_B(\mathbf{r})$ and $\psi(\mathbf{r}) = \phi_A(\mathbf{r}) + \phi_B(\mathbf{r})$. Furthermore, the volume fraction of the BCPs at the critical point of the macrophase separation, ψ_c, can be subtracted from $\psi(\mathbf{r})$, leading to a more convenient order parameter,[30] $\eta(\mathbf{r}) = \psi(\mathbf{r}) - \psi_c$. In terms of the two order parameters, ϕ and η, the model free energy of the AB–C blends can be written in the form,[30]

$$F[\phi,\eta] = F_S[\phi,\eta] + F_L[\phi,\eta] \quad (1)$$

where the short-range part F_S is the usual Ginzburg–Landau free energy, which is given by

$$F_S[\phi,\eta] = \int d\mathbf{r} \Big\{ D_1 \left[\nabla\phi(\mathbf{r}) \right]^2 / 2 + D_2 \left[\nabla\eta(\mathbf{r}) \right]^2 / 2 + f_\phi[\phi] + f_\eta[\eta]$$
$$+ f_{int}[\phi,\eta] \Big\}$$

$$\quad (2)$$

where the functions f_ϕ and f_η are specified by their derivatives such that $df_\phi/d\phi = -A_\phi \tanh\phi + \phi$, $df_\eta/d\eta = -A_\eta \tanh\eta + \eta$, respectively, where the coefficient A_ϕ/A_η tunes the micro/macrophase separation degree; and $f_{int} = b_1\eta\phi - b_2\eta\phi^2/2 + b_4\eta^2\phi^2/2 - b_3(\eta\phi^3 + \eta^2\phi + \eta^3\phi)$. Although the various parameters of the model are phenomenological in nature, they have unambiguous physical meanings as pointed out by Ohta and Ito.[30] The b_1 term is used to describe the short-range interactions between different species, and thus b_1 is expressed in terms of the interaction parameters $u_{ij}(i,j = A,B,C)$, $b_1 = (u_{AA} - u_{BB})/4 - (u_{AC} - u_{BC})/2$. The b_2 term induces the microphase separation that occurs in the copolymer-rich region, and the b_4 term regulates the microphase and macrophase separation. The ratio of b_2/b_4 is given by $\sqrt{N_C}/(\sqrt{N_{AB}} + \sqrt{N_C})$, where $N_{AB} = 2(1/N_A + 1/N_B)^{-1}$. The long-range term of the free energy F_L, which was originally proposed for AB diblock copolymers by Ohta and Kawasaki,[23] can be generalized to the AB–C system,

$$F_L[\phi,\eta] = \int d\mathbf{r} \int d\mathbf{r}' G(\mathbf{r} - \mathbf{r}') \{\alpha\delta\phi(\mathbf{r})\delta\phi(\mathbf{r}')/2 + \beta\delta\phi(\mathbf{r})\delta\eta(\mathbf{r}')$$
$$+ \gamma\delta\eta(\mathbf{r})\delta\eta(\mathbf{r}')/2\}$$

$$\quad (3)$$

where $\delta\phi = \phi - \bar{\phi}$ and $\delta\eta = \eta - \bar{\eta}$, and $\bar{\phi}$ and $\bar{\eta}$ are the spatial average of ϕ and η, respectively. The coefficients α, β, and γ are related to the polymerization N_A, N_B, and N_C, and satisfy the relationships of $\beta/\alpha = \gamma/\beta = (1/N_A - 1/N_B)/(1/N_A + 1/N_B) = (N_B - N_A)/(N_A + N_B)$.[30]

For the given free energy expressions, the ordering kinetics of the system is described by the TDGL equations,

$$\frac{\partial\phi}{\partial t} = M_1\nabla^2\frac{\delta F[\phi,\eta]}{\delta\phi} + \xi_\phi(\mathbf{r},t)$$

$$\frac{\partial\eta}{\partial t} = M_2\nabla^2\frac{\delta F[\phi,\eta]}{\delta\eta} + \xi_\eta(\mathbf{r},t),$$

$$\quad (4)$$

where M_1 and M_2 are two mobility coefficients, and ξ_ϕ and ξ_η are the random noise terms, which are given by $\xi_{\phi/\eta}(n,t) = B_{\phi/\eta}[\xi_{\phi/\eta,x}(n_x + 1, n_y, t) - \xi_{\phi/\eta,x}(n_x, n_y, t) + \xi_{\phi/\eta,y}(n_x, n_y + 1, t) - \xi_{\phi/\eta,y}(n_x, n_y, t)]$ in a lattice version, where $\xi_{\phi/\eta,x}$ and $\xi_{\phi/\eta,y}$ are random numbers uniformly distributed in the interval $[-1, 1]$ and $B_{\phi/\eta}$ is the noise amplitude.[24] Here we choose $B_\phi = B_\eta = 0.004$. A reasonably large amplitude of $B_{\phi/\eta}$ is needed to induce the spontaneous nucleation event.[31] Starting from the disordered phase, this set of kinetic equations is solved numerically in 2D to obtain the time evolution of the system. In particular, the nucleation and growth of the ordered cylindrical domains are obtained from numerical simulations.

3 Results and discussion

In our simulations, the model parameters are chosen as follows, $f = 0.4$, $D_1 = 0.5$, $D_2 = 1.0$, $M_1 = M_2 = 1.0$, $b_1 = -0.05$, $b_2 = 0.05$, $b_3 = 0.01$, $b_4 = 0.10$, $\psi_c = 0.20$, $A_\phi = 1.26$, $A_\eta = 1.10$, $\alpha = 0.02$, $\beta = 0.004$, and $\gamma = 0.0008$ ($\beta/\alpha = \gamma/\beta = 1 - 2f$).[30] The 2D simulation box is of the size 1000^2, corresponding to a few μm^2.[14] It should be noted that the negative b_1 indicates that the C-homopolymer is strongly selective to the B-blocks, thus the majority of the C-homopolymers will be located in the B-domains. The ratio of $b_2/b_4 = 1/2$ together with $f = 0.4$ determines $N_C = 0.48N$, i.e., the homopolymer is nearly half the length of the copolymer. With this choice of model parameters, the only free variable is the average volume fraction of the homopolymers, $\bar{\phi}_C$. Because the C-homopolymer is selective to the B-blocks, the phase behavior of the AB–C blend at small $\bar{\phi}_C$ is similar to the phase behavior of the AB–B blend investigated by Matsen.[32] Therefore we choose a smaller value of A_η than that of A_ϕ. In what follows we will restrict the value of $\bar{\phi}_C$ in the range between 0.01 and 0.10. When $\bar{\phi}_C$ is decreased from 0.10 to 0.01, the nature of the disordered phase changes from unstable, to metastable, and finally to stable. The ordered phase in the 2D model is the hexagonally packed cylindrical phase. The spacing, L_0, between two nearest-neighboring cylinders of the ordered cylindrical phase is determined to be $L_0 \approx 9.1$ lattice spacings.

The stability of the disordered phase is examined by computer simulations. For $\bar{\phi}_C > 0.05$, the disordered phase is unstable, as indicated by the observation that the cylindrical domains are formed immediately via spinodal decomposition after the sample is quenched from a disordered state to $\bar{\phi}_C > 0.05$. When $\bar{\phi}_C$ is decreased to $\bar{\phi}_C = 0.05$, a large number of nucleation events spontaneously occur at random positions in the sample, as shown in the snapshot at $t = 10\,000$ (Fig. 1(a)). This observation implies that the spinodal region of the disordered phase is located near $\bar{\phi}_C = 0.05$. After a further 10^4 time steps ($t = 20\,000$), the randomly distributed ordered domains have grown to fill the entire sample (Fig. 1(b)). It should be noted that the simulations were carried out in a 1024^2 box; for clarity, only a 512^2 portion of the sample is plotted in the figures. The Fourier transformation of the cylindrical structures shown in Fig. 1(b) is plotted on a logarithm scale in the inset. The circular scattering pattern is typical of a polycrystalline sample with a low degree of long-range order. In addition, the polycrystalline nature of the structure shown in Fig. 1(b) can be clearly visualized by the distribution of the orientational order parameter as defined in ref. 14. It has been demonstrated in our previous work that the ordering degree can hardly be improved by simple time evolution of the system, once the sample is trapped in the polycrystalline state.[14]

When the average homopolymer volume fraction $\bar{\phi}_C$ is decreased to $\bar{\phi}_C = 0.04$, the number of nucleations reduces tremendously, as shown by the snapshot at $t = 30\,000$ (Fig. 1(c)). The incubation time is much longer in this case, indicating a smaller nucleation rate. The smaller number of nuclei leads to a higher degree of ordering in the sample, as shown in the snapshot and its Fourier transformation at $t = 90\,000$ (Fig. 1(d)). With fewer nucleated ordered grains, the grown pattern has a higher ordering
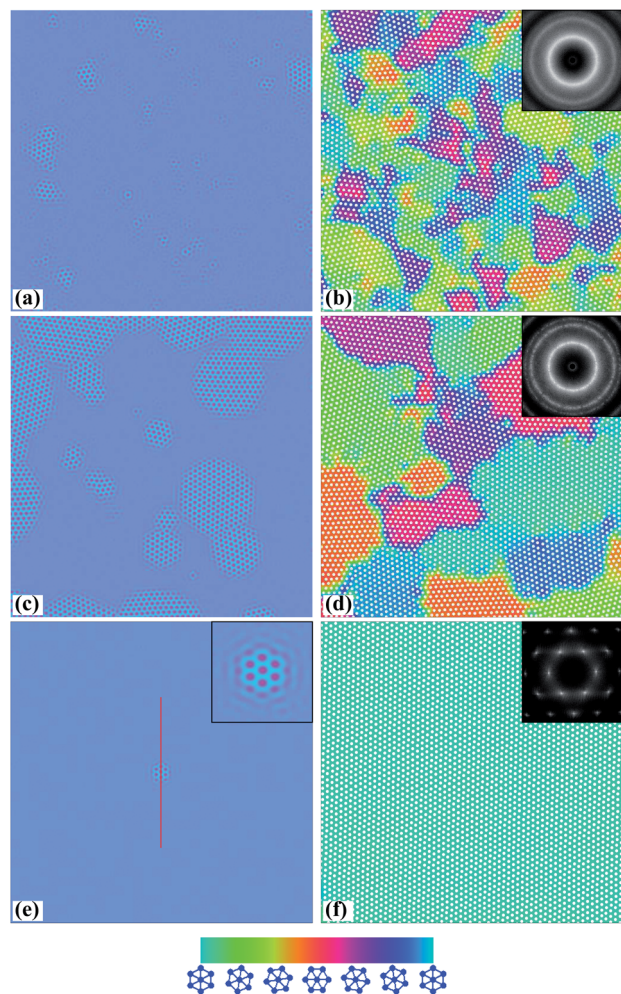
Fig. 1 Density configurations of A blocks for various values of $\bar{\phi}_C$: (a) $t = 10\,000$ and (b) $t = 20\,000$ for $\bar{\phi}_C = 0.050$; (c) $t = 30\,000$ and (d) $t = 90\,000$ for $\bar{\phi}_C = 0.040$; (e) $t = 185\,000$ and (f) $t = 340\,000$ for $\bar{\phi}_C = 0.030$. In the figures in the right column, the orientational order is indicated by the color spectrum, and the insets give the corresponding Fourier transformations. The solid line in (e) indicates the center of the nucleus.

degree, which is exhibited directly by the discontinuous circular pattern of the Fourier transformation in the inset of Fig. 1(d).

To suppress the homogeneous nucleation rate further, we decrease $\bar{\phi}_C$ to 0.03. In this case there is only one single nucleation event observed after a very long incubation time, as shown in (Fig. 1(e)) at $t = 185\,000$. This ordered domain is well maintained in the further growth process, leading to a single crystal sample at $t = 340\,000$ (Fig. 1(f)). The nature of the long-range order of this sample is indicated by the sharp Bragg peaks in the Fourier transformation of the structure. It is observed that, during the growth process, the ordered domain maintains a nearly circular shape, which is consistent with the theoretical prediction of Wickham et al.[26] For $\bar{\phi}_C \leq 0.025$, no spontaneous nucleation event is observed, thus the disordered phase becomes stable at $\bar{\phi}_C \leq 0.025$. Compared with the nucleation in pure diblock copolymers,[33] where the low nucleation rate is hard to obtain because of the tiny metastable region of the disordered phase and the order of the nucleated grains is not

well maintained during their growth, the small amount of homopolymers regulates the nucleation rate readily and significantly improves the isotropic property of an ordered domain during growth by its diffusion at the front of the grains where the phase separation occurs. The above shortcomings of the nucleation event in the pure diblock copolymers limit its application in the BCP lithography technique.

These simulations clearly demonstrate that the addition of homopolymers to the AB–C blends can be used to regulate the phase behaviour of the disordered phase and thus to control the homogeneous nucleation rate. The results also reveal the need to suppress the homogeneous nucleation rate for the production of single-crystalline samples. For the case of one-nucleus, the incubation time and the following growth time are very long. Therefore a better method is to introduce nucleation events by external potentials while keep the homogeneous nucleation suppressed.

Since homogeneous nucleation is a random process, the location and time of the nucleation event can not be predicted. On the other hand, in order to produce a single-crystalline sample, it is desirable to induce a nucleation event at a given time and a specified position. This can only be achieved via heterogeneous nucleation, in which a nucleus of the stable ordered phase is created by the presence of an external nucleation agent. The nucleation agents can be foreign dust particles, surfaces, or some features on an otherwise flat substrate. In what follows we will use a potential field on the substrate to model the nucleation agents.

To be specific, we will choose the system with $\bar{\phi}_C = 0.030$, corresponding to the case where the disordered phase is metastable and the system is located near the order–disorder transition (ODT). In this case the homogeneous nucleation is strongly suppressed, resulting in a very low nucleation rate and a very long incubation time. In order to design a nucleation agent for the system, it is informative to examine the properties of a critical nucleus. During the incubation time, the density is not uniform in the system.[20] This feature can be clearly seen by examining the density distributions of the polymers across a nucleus. Specifically, one-dimensional density distributions along the solid line at the center of the box in Fig. 1(e) for $t = 100\,000$ (black), $170\,000$ (red), and $185\,000$ (blue) are shown in Fig. 2. The density distributions in the disordered matrix at different times are indistinguishable.[20] In the early stages of
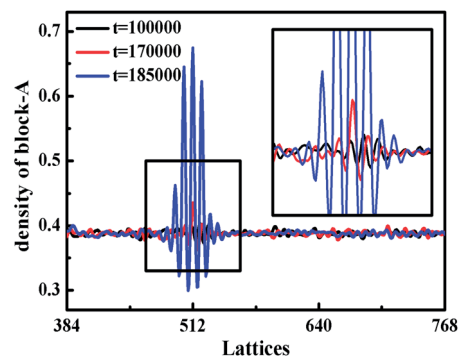

Fig. 2 One dimensional density distributions along the solid line at the center of nucleus in Fig. 1(e) at $t = 100\,000$ (black lines), $t = 170\,000$ (red lines), and $t = 185\,000$ (blue lines), respectively.

nucleation ($t = 170\,000$), an apparent peak at the centre of the nucleus can be clearly identified (see the red line in the inset). This feature indicates that the formation of a nucleus starts with a large fluctuation of the density distribution, forming a soliton-like wave packet at the nuclear center. This observation suggests that a nucleation agent can be modeled by a potential field that attracts the minority blocks to the center of the potential well, leading to the formation of a density peak. Motivated by this argument, we use a potential field of the form, $H_{\text{ext}}(\mathbf{r}) = -V_0/2\{\tanh[(-|\mathbf{r} - \boldsymbol{R_n}| + \sigma)/\lambda] + 1\}$, where $\boldsymbol{R_n}$ is the location of the nuclear center, and the physical meanings of other quantities can be found in ref. 14. These parameters are set as $\sigma = 0.15L_0$, $\lambda = 0.5$, and $V_0 = 0.04$. Our simulation results show that this particular potential field induces a cylinder of the minority blocks at the location of the nucleation agent as soon as the potential field is turned on. This induced cylinder can then act as the core of the nucleus, thus eliminating the incubation time. The efficiency of the nucleation agent is shown in Fig. 3, where the square root of the number of cylinders in the nucleated ordered domain is plotted as a function of time for the homogeneous and induced nucleation events. These results clearly demonstrate that the introduction of a nucleation agent eliminates the incubation time. At the same time the growth kinetics of the ordered domain is not affected by the presence of the nucleation agent. From these simulations, it can be concluded that a simple scheme to produce a single-crystalline sample is to quench the system to near the ODT so that homogeneous nucleation is suppressed. Then a nucleation agent is placed in the center of the sample to induce a nucleus, which will grow to occupy the entire sample. The limiting factor in this scheme is the time required for the central ordered domain to grow into the entire sample, which is limited by the diffusion of the materials.

In order to reduce the growth time and thus speed up the production time of large-scale ordered patterns, we can introduce multiple nucleation agents into the system.[7] These nucleation agents must be placed onto a periodic lattice which is commensurate with the symmetry and period of the ordered BCP structure. The multiple nucleation agents can be realized by a 2D periodic patterned substrate.
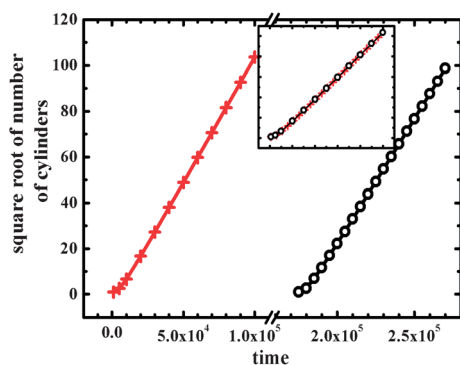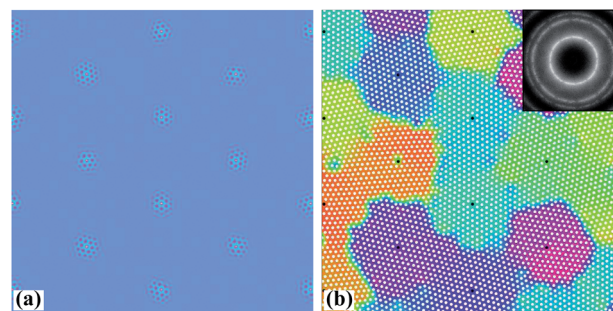

Fig. 4 Density configurations of the directed assembly of the copolymer–homopolymer blends with $\bar{\phi}_C = 0.030$ on the periodic single-spot fields with $L_s = 16L_0$ at: (a) $t = 6000$; and (b) $t = 160\,000$. The black spots indicate the locations of the field spots.

In our simulations, the substrate pattern is modeled by a hexagonally packed array of the potential wells with a period of L_s, which is chosen to be commensurate with L_0. The size of the simulation box is chosen to commensurate with L_s.[14] As an example, we choose $L_s = 16L_0$ which is much larger than those in experiments[7] or in our previous work.[14] The corresponding simulation box is 1019×1008. The simulated density profiles at an early stage of $t = 6000$ and a late stage of $160\,000$ are shown in Fig. 4. The results demonstrate that the growth of the ordered domains is well directed by the substrate pattern in that each potential well induces one ordered domain. These ordered domains grow to fill up the entire simulation box within a shorter time of about 2×10^4 as compared with that of about 10^5 in the single-nucleus case. In fact, as the macroscopic sample is much larger than the simulated box, the growing time is increased dramatically for the single-nucleus case. During the long period, it is hard to guarantee that no spontaneous nucleation events occur to destroy the structure order.

It is apparent that the ordered domains induced by the simple nucleation agents have random orientations, leading to a polycrystalline sample at the end of the growth process (Fig. 4(b)). The random orientation of the domains is due to the fact that the simple nucleation agent, in the form of a circularly symmetric potential well, does not control the orientation of the ordered domains. In order to utilize the full potential of multiple nucleation agents, it is essential to design a nucleation agent capable of controlling the position and orientation of an ordered domain.

The simple nucleation agent proposed above has circular symmetry, thus it is unable to control the orientation of the induced ordered domains. In order to control the orientation of the nucleus, the nucleation agent must be anisotropic, thus the single-site potential needs to be modified. We tested complex nucleation agents composed of 2 to 7 potential wells spaced at

Fig. 3 Square root of the number of cylinders in nucleation grains as a function of time. The unfilled circles and pluses indicate the results obtained from the spontaneous nucleation in Fig. 1(e), and from that induced by the nucleus agent of the field spot, respectively. The inset shows the comparison after a time shift.
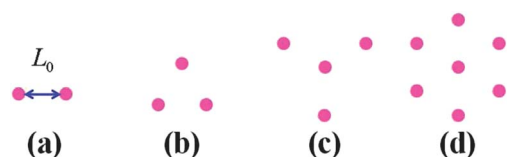

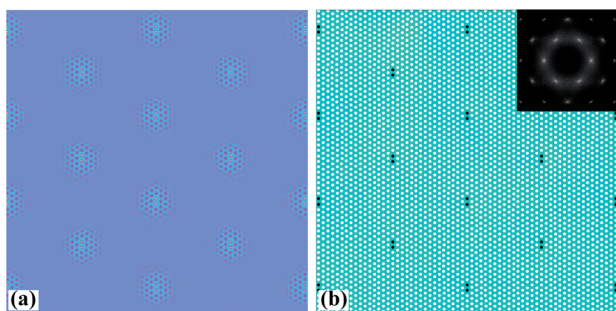**Fig. 5** Schematic plots of different units of nucleation agent.

Fig. 6 Snapshots of density configurations on the periodic double-spot fields with $L_s = 16L_0$ for $\bar{\phi}_C = 0.030$ at: (a) $t = 6000$; and (b) $t = 160\,000$.

equal distance L_0 as shown in Fig. 5, and the results demonstrated that all these anisotropic nucleation agents can be used to orient the induced ordered domains. In what follows we choose the simplest one, the double-spot potential, to illustrate the directing effect of the anisotropic nucleation agent. The simulated density plots at two times, $t = 6000$ and $t = 160\,000$ for $L_s = 16L_0$ are presented in Fig. 6. The results demonstrate that each double-spot potential has the capability to induce one nucleus at a given position and with a given orientation. Therefore the array of induced ordered domains are coherent in that their positions are commensurate with the ordered BCP phase and their orientations are uniform. The growth of these coherent ordered domains leads to the formation of a sample with long-range order, as demonstrated by the sharp Bragg peaks and the orientation distribution function (Fig. 6).

It is important to point out that, in order to obtain long-range ordered samples, homogeneous nucleation has to be suppressed, otherwise spontaneous nucleation will occur in the disordered regions. These incoherent nuclei would destroy the directed ordering process and form polycrystalline samples. Under the condition of $\bar{\phi}_C = 0.03$, we have observed that, for L_s as large as $64L_0$, the coherently placed anisotropic nucleation agents are still able to produce a single-crystalline sample. We did observe that, when the growing ordered domains just touch each other, the boundaries between the ordered domains exhibit some wavy features. However disclinations, in the form of five-fold or seven-fold defects, are rarely observed. The large-scale wavy boundaries can be annealed away quickly in the subsequent time evolution. The current results are very exciting because the DM in this case is $16^2/2 = 128$ for $L_s = 16L_0$ after being reduced by a factor of 2 due to the pair of field spots. This high DM is unprecedented, much larger than the high DM of 25–30 obtained from previous experimental and theoretical studies. Therefore, the new scheme of controlling nucleation rate, position and orientation simultaneously presents a technique which has the potential to increase the DM significantly. The 2D simulations for the ideal film system can be readily extended to 3D, where the film thickness can be considered. According to the equilibrium phase diagram of the AB–B blend calculated with SCFT by Matsen,[32] the ordered phase nucleated from the disordered phase should be a spherical phase in 3D space. However, the cylinder phase becomes stable instead of spherical when the film thickness is smaller than the nearest-neighbor spacing of
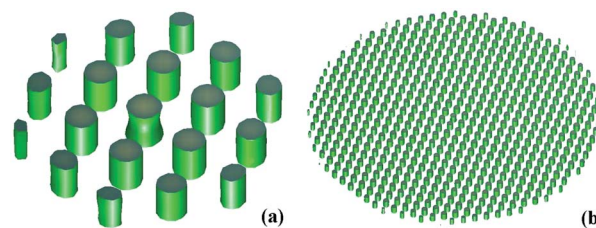

Fig. 7 Density-distribution snapshots of the isosurface for the induced single-nucleus case in 3D thin film with a thickness of $0.75L_0$ at two typical growing times of (a) $t = 10^4$ and (b) $t = 3 \times 10^4$.

domains.[34,35] As an example, we choose a film thickness of $h \approx 0.75L_0$, which corresponds to around 30 nm in the experimental sample of PS-b-PDMS with $f_{PDMS} = 16.5\%$ and the total molecular weight of 51.5 kg mol^{-1}.[7] The top and bottom surfaces of the thin films are chosen as neutral to get perpendicularly standing cylinders, and the reflective boundary conditions are used for the two surfaces in the 3D simulations. The density-distribution snapshots of the isosurface for the induced single-nucleus case, by a spot field imposed only on the bottom surface, at two typical growing times of $t = 10^4$ and $t = 3 \times 10^4$ in the 3D film are presented in Fig. 7. The snapshot at the early stage of nucleation in Fig. 7(a) clearly shows that the shape of the earliest-formed cylinder, induced by the nucleus agent on the bottom surface, does not have an ideal translational symmetry along the cylinder axis because of the field attraction.[7] Fig. 7(b) indicates that the neck shape of the cylinder is maintained during further evolution. When the periodic nuclei of the double-spot potential are applied, the perfectly ordered pattern is also readily produced in our 3D simulations.

The directing effect of various substrate-pattern periods of $L_s = 24L_0, 32L_0, 48L_0, 64L_0$ have been examined. In these systems, a small amount of defects are observed when the coherent ordered domains just merge to fill the sample. The defect concentrations obtained from averaging over eight independent samples for each L_s are $0.16 \pm 0.09\%$, $0.24 \pm 0.12\%$, $0.26 \pm 0.05\%$, and $0.23 \pm 0.07\%$, respectively. The dependence of the defect concentrations on L_s is weak. The small amount of defects can be easily annihilated because these defects are not clustered together to form a grain boundary. If the pattern unit is changed to be one of the more complex units in Fig. 5, the defect concentration becomes slightly lower for a given L_s.

4 Conclusions

In summary, a new scheme of producing large-scale ordered patterns from the directed self-assembly of block copolymers is proposed in theory. The scheme involves the control of intrinsic ordering kinetics coupled with the introduction of coherent multiple nucleation agents. First of all, a small amount of homopolymers are added to regulate the nucleation rate of the BCP self-assembly, and also to improve the domain order in the nucleated grains. Then multiple ordered domains are nucleated by introducing anisotropic nucleation agents into the system coherently, such that the orientation of all the domains are the same and the positions of the domains are commensurate with

the period of the ordered structures. At the same time, the homogeneous nucleation rate are suppressed so that spontaneous nucleation does not occur during the growth of the ordered domains. The mechanism and validity of this method are demonstrated by large-scale computer simulations on a model of diblock copolymer–homopolymer blends. With a proper choice of the system parameters and nucleation fields, the fabrication of perfectly ordered patterns with very high density multiplication has been demonstrated. Specifically, a DM value of 128 is achieved for a system with $L_s = 16L_0$, in which perfectly ordered BCP patterns are obtained after a growth time of the multiple ordered domains. For a system with $L_s = 64L_0$, a much larger DM (>2000) can be achieved after the small annealing time to eliminate the small amount of defects. These DM values are much larger than the highest DM of 25–30 from previous experiments and theory. Furthermore, the robustness of the proposed scheme is tested by our 3D simulations. Besides the possible applications for nanolithography, the underlying principles of phase-ordering kinetics obtained from the current study are readily applicable to any physicochemical systems undergoing first-order phase transitions.

Acknowledgements

References

1 M. Park, C. Harrison, P. M. Chaikin, R. A. Register and D. H. Adamson, *Science*, 1997, **276**, 1401.

2 R. Ruiz, H. M. Kang, F. A. Detcheverry, E. Dobisz, D. S. Kercher, T. R. Albrecht, J. J. de Pablo and P. F. Nealey, *Science*, 2008, **321**, 936.

3 T. Thurn-Albrecht, J. Schotter, G. A. Kästle, N. Emley, T. Shibauchi, L. Krusin-Elbaum, K. Guarini, C. T. Black, M. T. Tuominen and T. P. Russell, *Science*, 2000, **290**, 2126.

4 R. A. Segalman, H. Yokoyama and E. J. Kramer, *Adv. Mater.*, 2001, **13**, 1152.

5 S. O. Kim, H. H. Solak, M. P. Stoykovich, N. J. Ferrier, J. J. de Pablo and P. F. Nealey, *Nature*, 2003, **424**, 411.

6 M. P. Stoykovich, M. Müller, M. S. O. Kim, H. H. Solak, E. W. Edwards, J. J. de Pablo and P. F. Nealey, *Science*, 2005, **308**, 1442.

7 I. Bita, J. Yang, Y. S. Jung and R. A. Ross, *Science*, 2008, **321**, 939.

8 Y. Tada, S. Akasaka, H. Yoshida, H. Hasegawa, E. Dobisz, D. Kercher and M. Takenaka, *Macromolecules*, 2008, **41**, 9267.

9 J. Y. Cheng, C. T. Rettner, D. P. Sanders, H. C. Kim and W. D. Hinsberg, *Adv. Mater.*, 2008, **20**, 3155.

10 V. P. Chuang, J. Gwyther, R. A. Mickiewicz, I. Manners and C. A. Ross, *Nano Lett.*, 2009, **9**, 4364.

11 J. Xu, S. Park, S. Wang, T. P. Russell, B. M. Ocko and A. Checco, *Adv. Mater.*, 2010, **22**, 2268.

12 J. K. W. Yang, Y. S. Jung, J. B. Chang, R. A. Mickiewicz, A. Alexander-Katz, C. A. Ross and K. K. Berggren, *Nat. Nanotechnol.*, 2010, **5**, 256.

13 J. Feng, K. A. Cavicchi and H. Heinz, *ACS Nano*, 2011, **5**, 9413.

14 W. H. Li, F. Qiu, Y. L. Yang and A. C. Shi, *Macromolecules*, 2010, **43**, 1644.

15 Q. Y. Tang and Y. Q. Ma, *Soft Matter*, 2010, **6**, 4460.

16 J. W. Cahn and J. E. Hilliard, *J. Chem. Phys.*, 1958, **28**, 258; *J. Chem. Phys.*, 1959, **31**, 688.

17 G. H. Fredrickson and K. Binder, *J. Chem. Phys.*, 1989, **91**, 7265.

18 P. C. Hohenberg and J. B. Swift, *Phys. Rev. E: Stat. Phys., Plasmas, Fluids, Relat. Interdiscip. Top.*, 1995, **52**, 1828.

19 S. M. Wood and Z. G. Wang, *J. Chem. Phys.*, 2002, **116**, 2289.

20 T. Hashimoto and N. Sakamoto, *Macromolecules*, 1995, **28**, 4779; T. Hashimoto, N. Sakamoto and T. Koga, *Phys. Rev. E: Stat. Phys., Plasmas, Fluids, Relat. Interdiscip. Top.*, 1996, **54**, 5832.

21 H. J. Dai, N. P. Balsara, B. A. Garetz and M. C. Newstein, *Phys. Rev. Lett.*, 1996, **77**, 3677.

22 T. Q. Chastek and T. P. Lodge, *Macromolecules*, 2004, **37**, 4891.

23 T. Ohta and K. Kawasaki, *Macromolecules*, 1986, **19**, 2621.

24 Y. Oono and S. Puri, *Phys. Rev. Lett.*, 1987, **58**, 836; *Phys. Rev. A: At., Mol., Opt. Phys.*, 1988, **38**, 434.

25 M. Nonomura and T. Ohta, *J. Phys.: Condens. Matter*, 2001, **13**, 9089.

26 R. A. Wickham, A. C. Shi and Z. G. Wang, *J. Chem. Phys.*, 2003, **118**, 10293.

27 N. Y. Vaidya, C. D. Han, D. Kim, N. Sakamoto and T. Hashimoto, *Macromolecules*, 2001, **34**, 222.

28 V. R. Tirumala, V. Daga, A. W. Bosse, A. Romang, J. llavsky, E. K. Lin and J. J. Watkins, *Macromolecules*, 2008, **41**, 7978.

29 M. P. Stoykovich, E. W. Edwards, H. H. Solak and P. F. Nealey, *Phys. Rev. Lett.*, 2006, **97**, 147802.

30 T. Ohta and A. Ito, *Phys. Rev. E: Stat. Phys., Plasmas, Fluids, Relat. Interdiscip. Top.*, 1995, **52**, 5250; A. Ito, *Phys. Rev. E: Stat. Phys., Plasmas, Fluids, Relat. Interdiscip. Top.*, 1998, **58**, 6158.

31 The range of [0.001, 0.050] for the noise amplitudes has been examined for the observation of spontaneous nucleation events. The amplitude does not change the intrinsic characteristics of the nucleation events except that a larger amplitude just shifts the metastable region of the disordered phase toward a smaller concentration of homopolymer.

32 M. W. Matsen, *Macromolecules*, 2003, **36**, 9647.

33 L. R. Gomez and D. A. Vega, *Phys. Rev. E: Stat., Nonlinear, Soft Matter Phys.*, 2011, **83**, 021501.

34 H. Tan, Q. Song, X. Niu, Z. Wang, W. Gao and D. Yan, *J. Chem. Phys.*, 2009, **130**, 214901.

35 V. Mishra, G. H. Fredrickson and E. J. Kramer, *Macromolecules*, 2011, **44**, 5473.